JVI Accepted Manuscript Posted Online 2 August 2019
J. Virol. doi:10.1128/JVI.00907-19

GSK3732394: A multi-specific inhibitor of HIV entry

Running title: A Combinectin (combination adnectin) as a long acting inhibitor of HIV-1

David Wensel[1], Yongnian Sun[2], Jonathan Davis[2], Zhufang Li[1], Sharon Zhang[1], Thomas McDonagh[2], David Langley[2], Tracy Mitchell[2], Sebastien Tabruyn[3], Patrick Nef,[3] Mark Cockett[1] and Mark Krystal[1*]

[1]. ViiV Healthcare, Branford, CT, USA

[2.] Bristol-Myers Squibb, Wallingford, CT and Waltham, MA, USA

[3.] TransCure bioServices, Archamps, France

* Corresponding author: Mark.R.Krystal@viivhealthcare.com

Some of the data included in this manuscript was presented at the Conference for Retroviruses and Opportunistic Infections (CROI), February 22-25, 2016, Boston Massachusetts, Abstract 97.

Abstract

Long-acting antiretrovirals could provide a useful alternative to daily oral therapy for HIV-1 infected individuals. Building on a bi-specific molecule with adnectins targeting CD4 and gp41, a potential long-acting biologic, GSK3732394, was developed with three independent and synergistic modes of HIV entry inhibition that potentially could be self-administered as a long-acting subcutaneous injection. Starting with the bi-specific inhibitor, an alpha-helical peptide inhibitor was optimized as a linked molecule to the anti-gp41 adnectin, with each separate inhibitor exhibiting at least single digit nanomolar (or lower) potency and a broad spectrum. Combination of the two adnectins and peptide activities into a single molecule was shown to have synergistic advantages in potency, resistance barrier and in the ability to inhibit HIV-1 infections at low levels of CD4 receptor occupancy, showing that GSK3732394 can work *in trans* on a CD4+ T cell. Addition of a human serum albumin molecule prolongs the half-life in a human CD4 transgenic mouse, suggesting that it may have potential as a long acting agent. To show that, GSK3732394 was highly effective in a humanized mouse model of infection. GSK3732394 is currently in human studies.

Importance

There continue to be significant unmet medical needs for patients with HIV-1 infection. One way to improve adherence and decrease the likelihood of drug-drug interactions in HIV-1 infected patients is through the development of long acting biologic inhibitors. Building on a bi-specific inhibitor approach targeting CD4 and gp41, a tri-specific molecule was generated with three distinct antiviral activities. The linkage of these three biologic inhibitors creates synergy that offer a series of advantages to the molecule. The addition of human serum albumin to the tri-specific inhibitor could allow it to function as a long acting self-administered treatment for patients with HIV infection. This molecule is currently in early clinical trials.

Introduction

Antiretroviral drug discovery has evolved over the past decade. The availability of safe and effective single-pill regimens, first containing three or more antiretroviral agents and now containing two antiretroviral agents (1, 2) have shifted the discovery paradigm for new agents towards longer acting molecules that can potentially improve compliance, convenience and prophylaxis. Thus, a once monthly regimen of injectable cabotegravir/rilpivirine is currently in Phase 3 trials (3-5). Aside from small molecules, larger biologic molecules have many of the properties desired for a long acting agent. The first long-acting biologic for treatment of HIV, ibalizumab, has been approved for biweekly IV administration in highly treatment experienced (HTE) individuals (6) and PRO-140, a mAb targeted to the CCR5 co-receptor, remains in clinical trials (7).

The isolation and optimization of ever improving broadly neutralizing antibodies (bnAbs) to HIV-1 have opened up the possibility of their use for treatment and/or pre-exposure prophylaxis as long acting agents. However, even with the most improved bnAbs, breadth of activity remains an issue and models suggest that complete coverage would require multiple bnAbs to different regions of gp160 (8-12). This has led to the development of bi- and tri-specific molecules, whereby 2 or even 3 different bnAb specificities are combined into a single IgG-like molecule (13-15). This may reduce the number of molecules required for complete coverage of circulating HIV-1 viruses, although it does not solve the problem of pre-existing resistance to portions of these multi-specific molecules. In addition, targeting gp160 in a multi-specific biologic with a cell membrane-targeting moiety can greatly enhance the potency of an anti-HIV biologic. For instance, attaching an HIV-1 fusion peptide inhibitor to a monoclonal antibody targeting CCR5 (16), attaching a cholesterol moiety to the C-terminus of an HIV-1

fusion peptide inhibitor (17) or linking an HIV-1 fusion peptide inhibitor to various places on a neutralizing HIV-1 monoclonal antibody (18), are all means to localize the peptide at the surface of the target cell membrane, and all dramatically increase the potency of the combined molecule compared to the separate molecules. Also, bispecific antibodies consisting of anti-HIV-1 neutralizing antibody fragments targeting gp120 fused to ibalizumab or anti-CCR5 showed synergistic increases in potency compared to the individual inhibitors (18, 19), while fusion of a CD4-Ig molecule to a coreceptor-mimetic peptide provides greater potency, breath and a higher resistance barrier than broadly neutralizing antibodies (20, 21). Similarly, linking an adnectin targeting the CD4 molecule with another adnectin targeting the N17 region of gp41 produced a broad-spectrum inhibitor with enhanced potency (>500 fold), compared to the potencies of the individual adnectin components (22). Thus, localization of anti-HIV-1 entry inhibitors to the target cell surface through a variety of methods can significantly increase their local concentration at the site of action, thereby improving potency. GSK3732394 is a single biologic composed of 3 independent inhibitors of HIV-1 virus entry. One of the inhibitors is an anti-CD4 adnectin that drives synergistic potency of the other two anti-gp41 inhibitors (22) (an adnectin and a helical peptide inhibitor). Each inhibitor by itself has an extremely wide breadth of activity and should be active against the vast majority of circulating HIV-1 viruses. Thus, this single biologic molecule should not have the same issue of coverage as mixtures of bnAbs. However, a downside to any biologic modifier is the potential for an immunogenic reaction that effectively decreases the efficacy of the molecule. Although an adnectin is mainly derived from the 10th type III fibronectin domain of human fibronectin (23-26), the sequence variations needed to allow specific binding to a target may increase immunogenicity of the molecule. Previously, clinical studies with an adnectin (CT-322) targeting VEGRF-2 did induce an immunologic response in a

subset of individuals, although these anti-drug antibodies did not affect CT-322 plasma concentrations or VEGF-A biomarker responses (27). Clinical trials of GSK3732394 that are intended to determine the safety, pharmacokinetics, and immunogenicity profile of the molecule have recently initiated.

Results

Addition of a peptide fusion inhibitor to the bispecific inhibitor. Previously, we had described the creation and development of a potent HIV-1 entry inhibitor containing two independently generated adnectins targeted to either CD4 or the N17 region of gp41 (22, 28). Adnectins are small proteins based on the 10th type III domain of human fibronectin that can be subjected to *in vitro* selection to identify sequences with specific properties and can be thought of as similar to the VH portion of an antibody (23-26). In an attempt to further improve the virologic properties of this bi-adnectin inhibitor, a third inhibitory domain was added to the end of the anti-gp41 adnectin. This inhibitor is similar to the known fusion inhibitors developed for HIV-1, consisting of an α-helical peptide that binds at the amino terminus of the heptad repeat 1 of gp41 (29-31), upstream of where the anti-gp41 adnectin binds (22). The following considerations were employed in this inhibitor peptide design: optimal length; optimal positioning along gp41 relative to the anti-gp41 adnectin binding site; broad spectrum activity; potency; low predicted immunogenic risk; and biophysical behavior (minimal tendency to aggregate) in the context of an adnectin-peptide fusion. For a starting molecule we chose T-2635 (30), a sequence that was demonstrated to have stronger helical content, broader spectrum, and a higher barrier to resistance than enfuvirtide. However, T-2635 was designed to have a gp41 binding site shifted several helical turns to the C-terminus from that of enfuvirtide, including a

112 significant fraction of the N17 region. Theoretically, this would clash with the binding site of the
113 anti-gp41 adnectin. Therefore, designs with successive turns removed from the N-term of the
114 peptide (which bind the C-term end of the N17 adnectin binding site within gp41) were
115 generated.

116 Fusions of these peptides with a non-optimized member of the anti-gp41 adnectin family
117 and a non-HIV specific adnectin were produced and assayed for potency. It was believed that
118 this approach would best evaluate the potential for antagonism through binding competition and
119 synergy through potency improvements. An initial study was performed and showed that linkage
120 of the fusion inhibitor peptide can act synergistically when linked to an anti-gp41 adnectin.
121 Different length peptides linked identically to either an inert adnectin or the non-optimized anti-
122 gp41 adnectin 4773_A08 (22) were examined for inhibitory activity (Figure 1). Peptides of 30,
123 32 or 37 amino acids in length were linked to the carboxy terminus of the two adnectins with
124 identical linkers. The potencies of the peptides joined to the non-specific adnectin were inversely
125 correlated to the length, with EC_{50}s of >200 nM, 141 nM and 3.2 nM for the 30, 32 and 37
126 amino acid long peptides. Joining the 30 and 32 amino acid peptides to the anti-gp41 adnectin
127 produced synergistic potencies that were much stronger than either of the individual components.
128 Fusions to the longest peptide did not significantly increase the potency, as the EC_{50} for the
129 combination was 1.1 nM, while that of the peptide itself was 3.2 nM. Joining the peptide with
130 the anti-gp41 adnectin has a large synergistic effect on potency when the inhibitors are relatively
131 weak, but the effect may be less pronounced when at least one of the inhibitors is optimized for
132 stronger binding. Therefore, additional optimization work was carried out with shorter, weaker
133 peptides so that improvements in potency and synergy could be more readily seen.

The sequence of the peptide was further optimized by using structural models, which identified nine amino acids that were likely to point into solvent when the peptide is bound. Starting with a protein which consists of an inert adnectin fused to a shortened peptide fusion inhibitor (PRD-1022; Supplemental Table 1), a small library was generated from oligos with degenerate positions, such that in each member of the library, one of the nine positions was randomized. The peptide with the nine randomized positions underlined is: SRIEALIRAAQEQQEKNEAALRELDKWAS. One hundred sixty-three separate sequences were expressed and tested for potency. Most of the positions did not show any improvement upon mutation (not shown), but the Asp residue (***D***KWAS) was profoundly sensitive to changes, showing improvements of up to 50-fold when mutated to hydrophobic residues larger than valine (Figure 2) (32, 33). A tyrosine was chosen in the final construct based upon the high potency and the biophysical properties of the adnectin-peptide molecule. Adding the optimal N-terminal sequence element into this peptide gave the sequence ultimately used in our clinical candidate, GSK3732394: TIAEYAARIEALIRAAQEQQEKNEAALRELYKWAS.

Antiviral properties of the peptide fusion inhibitor: The 35 amino acid sequence was made into a standalone peptide (named 203613-24) in order to measure its potency and binding characteristics. Because a glycine-based linker would ultimately be used to connect this peptide to an anti-gp41 adnectin, the 203613-24 synthetic peptide included an additional glycine residue in the N-terminal position to provide a similar context. The antiviral potency of this isolated 36-amino acid peptide was measured in a multiple cycle experiment against a luciferase-expressing NL_{4-3} virus. 203613-24 exhibited sub-nanomolar inhibition, with an EC_{50} of 0.40 $\pm$ 0.27 nM (Table 1). The molecule also showed no cytotoxicity in cell culture against MT-2 cells, with a CC_{50} of >10,000 nM. In order to assess the binding of the isolated peptide component to gp41,

we designed a 5-helical bundle protein (PRD-828; Supplemental Information) using the sequences from gp41 that are thought to contact the peptide. The single chain molecule has all three inner helices, and two of the outside helices with connecting linkers, leaving one outer slot open for the peptide to bind. Biotinylated PRD-828 was captured onto a neutravidin-coupled surface of a CM5 Biacore T200 SPR chip, and the 203613-24 peptide was flowed over in solution at various concentrations. The peptide exhibited binding to the artificial gp41-like trimer substrate, with a k_a of 2.3 x 10^6 (1/Ms), a k_d of 2.5 x 10^{-4} (1/s) and a K_D of 0.1 nM (Table1). Experiments were conducted under physiological buffer conditions and temperature (37°C).

Resistance to the isolated peptide inhibitor: In order to select viruses resistant to 203613-24 in cell culture, MT-2 cells were infected with NL_{4-3} virus in the initial presence of a 2X EC_{50} concentration (~0.8 nM) of the peptide and passaged in increasing concentrations of inhibitor. C. Virus with decreased susceptibility to the peptide was identified at passage 11 (33 days in culture) at a final peptide concentration of 0.51 μM. The virus population at passage 11 was examined and found to have a reduced susceptibility to 203613-24 of ~18-fold. Population sequencing of the virus stocks identified a single amino acid change of V549A (V38A when amino acid numbering is initiated at gp41) compared to the control virus. This amino acid is within the proposed binding site for the peptide, thus confirming the target of the inhibitor. Even though the sequences of 203613-24 and enfuvirtide are different, it has been reported that this V549A substitution is selected by enfuvirtide and is a common clinical resistance mutation (34). Given this overlap with a known enfuvirtide resistance mutation, we examined 5 additional known enfuvirtide resistant mutations for their effect on peptide susceptibility. Table 2 shows that the peptide retains good activity against most of these enfuvirtide resistant mutations, exhibiting a reduced susceptibility only to V549A (V38A), and even in this case, enfuvirtide has

an order of magnitude greater fold change in response to the V38A mutation. Thus, although the peptide exhibits some cross-resistance to enfuvirtide resistance mutations, it tends to exhibit a more restrictive and potent profile.

Creation of a tri-specific inhibitor. The length of the G_4S-based linker used to connect the peptide to the carboxy end of the anti-gp41 adnectin was then optimized as described in Table 3. As done previously, a shortened, weaker form of the peptide was used to more readily observe changes in synergistic potency. Adnectin-peptide fusion constructs were made with (G_4S)-based linkers. We hypothesized that linker length may affect the synergy between the adnectin and peptide, and that the C-terminal residues of the adnectin could also affect the synergy. Therefore, a series of molecules was made with different carboxy termini on the adnectin (4773_A08), and with different linker sequences. Table 3 shows the sequences of the adnectin C-terminus, linker, and peptide used. Based upon these data, the C-terminus of the anti-gp41 adnectin in the final molecule was altered to NYRTP and the linker sequence used was GGGGSGGGGSGGGGSGGGG ($[G_4S]_3G_4$).

The potencies of the individual inhibitors, combinations of two inhibitors, and the tri-specific inhibitor (all are the made from the final optimized adnectins and peptide) are shown in Table 4. A non-HIV specific adnectin was used to substitute for either the anti-CD4 or anti-gp41 adnectins in some of the constructs in order to retain the molecular geometry and context, while allowing the dissection of the relative contributions of the individual inhibitors to potency. The linker sequences used were also the optimized linkers from the final tri-specific molecule (full sequences of each molecule are shown in Supplemental Table 3). Addition of an inert adnectin in tandem with an optimized, active adnectin (X_41_ and C_X_, where X is the non-specific adnectin, C the anti-CD4 adnectin and 41 the anti-gp41 adnectin) decreased the potency of the

active moiety (~5.6-fold for the anti-CD4 adnectin and ~21.6-fold for the anti-gp41 adnectin), while having the two active moieties (C_41) synergistically increased potency to 0.02 ± 0.01 nM (22). Interestingly, addition of the peptide to the bi-specific adnectin molecule drops the EC_{50} ~4X to 0.09 ± 0.01 nM. Good activity is also observed when the non-specific adnectin is swapped for the anti-gp41 adnectin in the presence of the two other inhibitors (C_X_P, where P is the peptide 203613-24; EC50 + 0.21 ± 0.03 nM)), but the potency dropped ~10-fold compared to the C_41_P optimized inhibitor.

Addition of a PK-enhancing element to create the final GSK3732394 molecule: Although the tri-specific molecule is highly potent, for it to be useful as a long-acting antiviral agent, it needs to have a long intrinsic half-life *in vivo*. Probably as a consequence of their small size, adnectins by themselves are known to have a short half-life *in vivo*, likely due to renal clearance (35). Thus, a pharmacokinetic enhancer (PKE) was required to improve the intrinsic *in vivo* half-life of these molecules. After examining the biophysical, antiviral and PK effects of inserting several different PKE elements at different sites in the molecule, a human serum albumin (HSA) molecule was added to the amino terminus of the anti-CD4 adnectin via a 25-amino acid linker. The resulting molecule is GSK3732394 (formerly BMS-986197) (Table 4), whose sequence is shown in Figure 3.

The effect of adding the human serum albumin on antiviral activity was addressed using two different molecular constructs. One molecule (C_41_P) is the exact match to GSK3732394 except that it is missing the HSA molecule and linker sequence connecting it to the anti-CD4 adnectin. It exhibited an EC_{50} of 0.09 ± 0.01 nM. The final tri-specific molecule, GSK3732394, exhibits an EC_{50} = 0.27 ± 0.17 nM (Table 4). Thus, the addition of HSA to the amino terminus of a 3-component molecule maintains good potency, but does decrease it by ~3-fold in the context

of C_41_P. In addition, the cytotoxicity of the molecule was examined using an XTT method. There was no cytotoxicity observed up to the highest concentration of GSK3732394 tested (>2.9 μM). Given that the assay measures the metabolism of XTT by mitochondrial enzymes, this suggests that at the concentrations tested, GSK3732394 is neither cytotoxic nor cytostatic. Finally, serum binding effects on the potency of GSK3732394 were examined with the addition of 40% human serum. The EC_{50} and EC_{90} values in the presence of human serum were within 2-fold of their values without human serum (EC_{50} fold change: 1.14 $\pm$ 0.64; EC_{90} fold change: 1.29 + 0.28). Thus, the presence of human serum does not have a significant effect on the potency of GSK3732394.

Binding affinities of inhibitors in the context of GSK3732394 compared to isolated inhibitors: In order to examine whether the binding of GSK3732394 to its targets differed from its individual components, the affinity of GSK3732394 was measured by SPR against the 3 targets used for analysis against the individual components (22, 28). Thus, binding of GSK3732394 was measured against human CD4 protein, the N17 containing peptide trimer IZN24 (22) and the 5-helical bundle reagent containing the target for the fusion peptide inhibitor (PRD-828). All experiments were conducted under physiological buffer conditions and temperature (37°C). The results are shown in Table 5. The K_D of binding to CD4 is 27-fold weaker with GSK3732394 than with 6940_B01 (the anti-CD4 adnectin), due primarily to a slower on-rate. This result correlates data showing that addition of HSA appears to reduce potency (Table 4). However, CD4 binding could also be affected by the linkage of the anti-gp41adnectin and/or the fusion peptide inhibitor.

The K_D for binding of GSK3732394 to IZN24 was 4-fold weaker than the binding of the isolated anti-gp41adnectin (6200_A08) to IZN24. It is possible that steric hindrance resulting

249 from attaching the HSA and anti-CD4 adnectin to the anti-gp41adnectin may adversely affect
250 interaction with gp41. Similarly, the binding affinity of GSK3732394 for PRD-828 was 3- to -4-
251 fold weaker than the affinity of the isolated peptide component for the same target. Thus, linking
252 the components together into a single molecule does result in decreased binding to their specific
253 targets. However, that is compensated for by the synergies associated with the linkages, which
254 results in increased potencies.

255 **High potency of the GSK3732394 at low receptor occupancies:** From the antiviral potency
256 and the SPR affinity data (Tables 4 and 5), it is clear that fusing the anti-CD4 adnectin
257 (6940_B01) to HSA and to the anti-gp41 adnectin (6200_A08) plus the peptide in the context of
258 GSK3732394 has a detrimental impact on the binding of 6940_B01 to CD4, manifested
259 primarily as a slower on-rate. To study this effect further, the isolated anti-CD4 adnectin
260 (6940_B01) and GSK3732394 were assessed for their ability to compete with fluorescently
261 labeled 4945_G06 for binding to CD4 on the surface of MT-2 cells. 4945_G06 is a progenitor of
262 6940_B01 that differs slightly from it, but these differences do not affect the potency of the
263 molecule or its ability to compete with 6940_B01 for binding to CD4 (28). MT-2 cells are used
264 for antiviral EC_{50} determinations, so the binding affinity can be directly compared with antiviral
265 potency. A dose response curve for binding to human MT-2 cells was generated with the
266 4945_G06 molecule and compared with the dose response curve for antiviral potency of this
267 molecule (Figure 4). The EC_{50} for binding to MT-2 cells is 7.0 nM while the EC_{50} for antiviral
268 activity in MT-2 cells is similar (4.9 nM). More importantly, the dose response curves for the
269 two activities with the isolated anti-CD4 adnectin were similar and almost super-imposable. This
270 indicates that antiviral potency of the individual adnectin is directly related to binding (in a 1:1

fashion) and suggests that saturation of binding to CD4 with the anti-CD4 adnectin as an individual inhibitor must be accomplished in order to obtain complete inhibition of infection.

When GSK3732394 was used to generate a dose response curve for binding to MT-2 cells, the binding was weaker to cells compared to 6940_B01. The binding was 100-fold weaker, with an EC_{50} of 200 nM. However, the dose response curve of antiviral activity of GSK3732394 in MT-2 cells is ~4 log_{10} stronger compared to CD4 binding and >2 log_{10} better than the antiviral activity of 4945_G06 in these MT-2 cells. This suggests that the antiviral activity of GSK3732394 is potent at relatively low receptor occupancy (RO). Further experiments at lower concentrations show that at an EC_{50} (0.27 nM) concentration of GSK3732394 in cell culture, only ~0.2% of CD4 molecules on MT-2 cells are bound to GSK3732394, while at an EC_{90} concentration of 2 nM, ~1.5% of CD4 receptors are bound to GSK3732394 (data not shown). Thus, potent antiviral activity is observed at relatively low receptor occupancy of the inhibitor on CD4 on the surface of cells. Similar values for cell binding were generated for both the individual adnectin and GSK3732394 using human PBMCs (not shown).

Selection of GSK3732394 resistant virus in cell culture: In order to select viruses resistant to GSK3732394 in cell culture, MT-2 cells were infected with NL_{4-3} virus in the initial presence of a 2X EC_{50} concentration (~0.5 nM) of GSK3732394. Drug concentration was progressively increased until reaching 300 nM, then was kept constant at that level through multiple passages. NL_{4-3} virus was also passaged concurrently without GSK3732394 selection as a control. Virus growth was observed to be slower in the GSK3732394 selection sample, and 37 passages (175 days in culture) were required for the virus to grow well enough to warrant harvesting. At that time, the virus population was examined and found to have an 18-fold reduced susceptibility to GSK3732394. Population sequencing of the virus stocks identified 7 amino acid changes in

294 gp160 compared to the control virus (Figure 5). Five of these changes were in the gp120 region,
295 with two (T138I and N301K) destroying potential N-linked glycosylation sites (PNGS). The
296 N301K change was also observed during selection with 6940_B01 (28). There is an additional
297 PNGS located between amino acids 396 and 401; the F396S and S401T mutations may have
298 affected the glycosylation occupancy of this site as well. Previous resistance selection using
299 6940_B01 showed that resistance mapped to the loss of glycosylation sites in gp120, similar to
300 that observed with ibalizumab (36). In addition to the changes in gp120, a Q577R substitution
301 was observed in the N17 region. This same change was selected by the anti-gp41 adnectin alone
302 and should render the virus resistant to the individual 6200_A08 component (22). Finally, an
303 L544S substitution was observed in the proposed region targeted by the peptide inhibitor. No
304 other changes were observed in gp160. Recombinant virus containing a gp160 gene with all 7 of
305 these substitutions exhibited a 60-fold loss in susceptibility to GSK3732394. The virus was
306 growth impaired, similar to that observed with the earlier Q577R virus alone (22).

307 Virus populations from approximately every third passage from the selection were
308 collected and viral RNA was purified from a portion of the viral supernatants. The genomes were
309 then population sequenced, while the remaining supernatants were examined for susceptibility to
310 GSK3732394. As can be seen from Figure 5, the N301K mutation occurred first at ~30% in
311 passage 9, and it was fixed at ~100% by passage 12. At this passage, the Q577R mutation was
312 first observed in a small percentage of genes (~20%) and was fixed at ~100% by passage 24.
313 Also, at passage 24, all of the other gp120 substitutions were fixed, but the fold-change (FC)
314 associated with this virus was still low. The appearance of the L544S substitution (~50%) at
315 passage 33, which was fixed by passage 37, corresponded to the first significant FC of ~18.
316 Thus, a larger FC was observed only when resistance to both anti-gp41 inhibitors emerged.

GSK3732394 retains activity against virus resistant to components of the GSK3732394 molecule: A potential advantage of joining the individual inhibitor components into a single molecule may be an effect on the resistance barrier compared to the individual components. This was examined using recombinant viruses that contain resistance-inducing mutations to one or more of the individual inhibitors. Recombinant envelope proteins resistant to each of the individual adnectins have been described and were selected above (22, 28), and additional recombinant viruses with resistant mutations to two components (either against the anti-CD4 adnectin + anti-gp41 adnectin, anti-CD4 adnectin + peptide or anti-gp41 adnectin + peptide) were constructed and tested. The results of these *in vitro* studies are shown in Table 6. As expected, the individual components exhibited higher fold-changes against the viruses containing their selected substitutions but were fully active against recombinant viruses containing the resistance-inducing substitutions to the other components. Importantly though, the full length GSK3732394 did not exhibit a noteworthy FC against any of the 3 viruses resistant solely to one of the components. The only viruses where a large FC was observed included both anti-gp41^{R} + peptide^{R} substitutions. Interestingly, in separate experiments, the tri-specific molecule (C_41_P; Table 4) that is missing the human serum albumin molecule and linker was examined against additional recombinant viruses (Table 6) that contained resistance mutations to the anti-CD4 adnectin and either the anti-gp41 adnectin or the peptide. As with GSK3732394, a high fold change was observed against virus with resistance to the two gp41 targets (FC = 125), but when examined against either the anti-CD4^{R} + peptide^{R} or anti-CD4^{R} + anti-gp41^{R} viruses, full susceptibility was observed (0.3- and 0.4-FC, respectively). This suggests that the enhanced potency in the molecule is being driven mainly by the activity of the gp41 inhibitors, presumably as a result of targeting to the cell membrane through CD4 binding. This demonstrates that joining

340 the components in a single molecule could overcome resistance to any one component, as well as
341 to some of the dual resistant combinations, which suggests that another property of joining the
342 inhibitors into one molecule may be to raise the resistance barrier of the GSK3732394 molecule
343 compared to those of the individual components.

344 **Breadth of antiviral activity:** Previously, a cohort of 124 functional envelope gene populations
345 were used to examine the spectrum of activity for the individual adnectin inhibitors in a cell-cell
346 fusion assay (22, 28). This same cohort was used to analyze the breadth of activity of the
347 GSK3732394 biologic molecule. This assay usually shows greater run-to-run variability than an
348 infectious virus assay, so the results are normalized against an LAI envelope clone and expressed
349 as fold-change.

350 The 124 envelope gene populations were derived mainly from clinical samples and span
351 11 different HIV-1 subtypes (22). Figure 6 shows the FC of the cohort compared to the LAI
352 envelope. GSK3732394 was active against 100% of these envelopes. Of the 124 gp160
353 populations, only 2 envelope proteins exhibited an FC >10 in this assay. All 64 subtype B
354 envelope proteins and 26 subtype C envelope proteins exhibited little to no fold change in the
355 assay. The only two envelope proteins to exhibit a >10 FC were both from subtype D (11.5-FC
356 and 17.3-FC), while 2 other subtype D envelope proteins showed no significant FC. When the
357 population of envelope genes from one of these subtype D viruses was cloned into recombinant
358 virus, it exhibited an FC compared to the control virus of 13.3. When the envelope gene from
359 this subtype D virus was sequenced, Q577K and L544V substitutions were observed, which
360 could impact the anti-gp41 adnectin and peptide inhibition and account for the FC seen in this
361 virus. Cloning of the other subtype D envelope did not produce an infectious virus, and
362 sequencing of the gp160 gene did not identify mutations that were likely to impact the anti-gp41

363 inhibitors. When envelope gene populations exhibiting the next highest FCs of 6 or 5.8 were
364 cloned into recombinant viruses and examined against GSK3732394, the FCs were 1.7 and 0.7,
365 respectively. This suggests that all other envelopes are highly susceptible to GSK3732394. Thus,
366 this cell-cell fusion data demonstrates that the GSK3732394 molecule is highly active against the
367 vast majority of virus envelope proteins, including all 90 of the envelope proteins examined from
368 the major subtypes B and C.

369 To confirm the breadth of activity of GSK3732394, it was further examined against a
370 series of primary clinical isolates. A panel of 19 HIV-1 clinical isolates from various Group M
371 subtypes (including subtypes A, B, C, D, F, G and CRF01_AE) and 1 virus each from Group N
372 and Group O were evaluated in dose response experiments. GSK3732394 was active against all
373 the clinical isolates, with EC_{50}s ranging from 0.10 nM to 2.1 nM. (Table 7), confirming the wide
374 spectrum of activity of GSK3732394.

375 **Activity of GSK3732394 in a humanized mouse model of infection.** In order to examine the
376 potential of GSK3732394 to inhibit virus *in vivo*, a human immune system was reconstituted in
377 NOG mice with hematopoietic stem cells isolated from human cord blood (37). After 14 weeks
378 of engraftment, mice were infected with the YU2 strain (R5 tropic) via IP injection. Table 8
379 shows the activity of the various individual components and GSK3732394 against YU2 virus in
380 cell culture. All molecules were active against this virus, although the potency was slightly
381 decreased compared to NL_{4-3} (Table 4). At Day 37 post infection, mice were analyzed for viral
382 load and evenly distributed into 5 groups of 8 mice each. Viral loads of most mice at the time of
383 GSK3732394 administration were in the 10^5-10^6 c/mL range. One group was treated
384 subcutaneously (SC) with vehicle only, while one group was given a regimen of RAL + TDF +
385 FTC daily incorporated in the food pellet. Based on an average consumption of 4 g of food per

386 day, each animal received daily 2.4 mg of TDF, 2.35 mg of FTC and 19.2 mg of RAL. The other
387 3 groups were treated with GSK3732394, injected SC every 3 days at doses of 4, 12.5 or 32
388 mg/kg. Every 9 days (every third dose) prior to dosing, blood was taken for viral load and other
389 analyses. The study lasted approximately 2 months (63 days), after which treatment was stopped.
390 At this point, most animals were exsanguinated, with the exception of three animals each in the
391 ARV treated group and the 32 mg/kg GSK3732394 treated group. These animals were left
392 untreated for an additional 21 days (with blood taken 9 days after treatment termination and at
393 end of study) to probe virus rebound. Treatment with GSK3732394 was generally safe and well
394 tolerated. Although some mice died during the two-month course of the study, more died in the
395 vehicle and ARV groups (3 and 2 mice, respectively) than in the GSK3732394 treatment groups
396 (1 each of the 4 and 32 mg/kg treatment groups).

397 The receptor occupancy of GSK3732394 on CD4 was measured every 9 days (Figure 7a).
398 Variability was observed within each cohort, but a clear dose dependent increase in RO is
399 observed, with the RO among animals in each cohort falling within a ~20% range. The 4 mg/kg
400 dose produced the lowest RO, between a few percent and ~25% at each time point, while the 32
401 mg/kg dose exhibited ROs between ~40-60% at the various time points. The 12.5 mg/kg dose
402 was intermediate with respect to RO (~20-40%).

403 As expected, the plasma concentrations of GSK3732394 correlated with the RO values
404 (Figure 7b). A dose dependent increase in plasma concentrations was observed and remained
405 consistent throughout the study. There was greater variability in the plasma concentrations at the
406 highest dose compared to the lower doses, especially the 4 mg/kg dose.

407 A summary of the average viral loads for each group at the indicated time points are
408 shown in Figure 8. Interestingly, the vehicle cohort saw approximately a 1 log increase in viral

409 titers over the 2 months of the study, while all the inhibitor-treated samples exhibited viral load
410 declines. The data show that at all doses tested, GSK3732394 treatment resulted in significant
411 reductions in viral loads. This even includes the lowest dose cohort (4 mg/kg), which averaged
412 relatively low CD4 receptor occupancy at trough (Figure 7) throughout the study. In the
413 GSK3732394 treated cohorts, a dose dependent decline in viral load was observed, with the
414 highest dose seeing almost a 4 $\log_{10}$ drop over the course of the study compared to titers at the
415 start of the experiment. However, all three GSK3732394 treated dose cohorts tended to show an
416 increase in viral load beginning from Days 36 - 45 until the end of the study. Thus, by Day 63, the
417 average viral load decline was over 3 $\log_{10}$ for the 32 mg/kg group and slightly lower and higher than 1
418 $\log_{10}$ for the 4 and 12.5 mg/kg groups, respectively. In addition, there were mice in certain groups
419 whose viral loads were below quantitative levels at certain times. These are indicated by the numbers
420 shown in Figure 8. Thus, 6/8 animals had undetectable viral titers by Day 36 in the 32 mg/kg group,
421 while by Day 63 it was 4/7 animals, while 2/8 animals in the 12.5 mg/kg group possessed viral loads
422 below detectable levels at Day 63. By that time, all animals in the ART group (6/6) had undetectable
423 viral loads.

424 At Day 63, the study was terminated for most mice and plasma was collected from all mice but
425 3 mice each in the ART treated and 32 mg/kg treated cohorts. Plasma samples were taken from all
426 mice in the 4 mg/kg dose cohort and 7 mice in the 12.5 mg/kg dose cohort that exhibited
427 measurable viral titers at Day 63, along with 4 mice from the highest 32 mg/kg dose cohort with
428 viral titers. The gp160 genes were amplified from plasma virus by RT-PCR and the gene
429 products were population sequenced. Amplification was successful in most cases, except for one
430 animal in each of the dose groups. In all samples at Day 63 except one, only one amino acid
431 substitution was observed within the gp160 gene. This was a Q577R change within the N17

region of gp41. The only sample without this change came from the one mouse in the 32 mg/kg cohort whose titer at Day 63 was below the level of quantitation but had an amplifiable gp160. This mouse contained the wild type Q577 and no other changes. The Q577R mutation was previously shown to elicit resistance to the anti-gp41 adnectin that is part of GSK3732394 (22).

Thus, in a humanized mouse model of infection, GSK3732394 was able to significantly reduce virus titers, even at relatively low CD4 receptor occupancies. Over time, breakthrough of viruses occurred, and the durability of response was dose dependent over the two-month long duration of the experiment. Breakthrough viruses contained a selected mutation that engendered resistance to the anti-gp41 adnectin portion of GSK3732394.

Three mice without measurable viral titers in the highest dose group of 32 mg/ml and 3 mice in the ART treatment group were continued on study without drug for an additional 21 days after Day 63, with plasma taken 9 days after treatment termination (Day 72) and at end of study. Viral titers were measured at both time points, although there was only enough plasma available for analysis at the Day 72-time point. In the ART treatment group, one sample (either Day 72 or Day 84) of each of the animals showed a measurable viral titer, while all three animals in the 32 mg/kg GSK3732394 treatment group rebounded to titers similar to that observed at start of GSK3732394 treatment. Plasma samples from Day 72 of these 3 mice were amplified and the gp160 gene was population sequenced. In these samples, two mice contained virus with a wild type Q577, while one mouse contained virus with a Q577Q/R mixture.

Discussion

Previously, we described a bispecific inhibitor comprised of an anti-CD4 adnectin (28) linked to an anti-gp41 adnectin targeting the N17 region of gp41 (22). The linkage was

455 optimized so while each individual inhibitor possessed single-digit nM EC_{50} potency, the
456 connected molecule was >100-fold more potent than the mixture of the two (22). However,
457 studies suggested that the anti-gp41 adnectin suffered from a relatively low resistance barrier. To
458 address that deficiency and potentially make the molecule effective enough that it could become
459 a long acting anti-retroviral agent, an anti-gp41 antiviral peptide was linked downstream of the
460 anti-gp41 adnectin targeting a region in gp41 similar to enfuvirtide. Addition of the peptide did
461 decrease the potency of the molecule (from 0.02 to 0.09 nM) but improved the resistance barrier
462 of the combined molecule by making the molecule fully active against viruses resistant to one of
463 the components.

464 Once a tri-specific inhibitor was constructed, the next stepping stone was to improve the
465 half-life of the molecule to enable it to be administered less frequently than once daily.
466 Adnectins by themselves tend to have short half-lives in humans (35, 38), so a pharmacokinetic
467 enhancing (PKE) molecule needed to be included in the final molecule. After analyzing multiple
468 formats, a human serum albumin molecule placed at the amino terminus was chosen as the PKE
469 element. The final molecule GSK3732394 exhibited an EC_{50} of 0.27 $\pm$ 0.17 nM, which is ~3-fold
470 weaker than the molecule without the PKE element, perhaps due to weaker affinity for CD4
471 when the HSA molecule is present. GSK3732394 was active against all viruses and viral
472 envelope proteins in the experimental panel. There was one subtype D virus envelope protein
473 that showed a ~17.3-FC in potency in a cell-cell fusion assay compared to the control. Upon
474 sequence analysis, this envelope protein possessed mutations (Q557K and L544V) that could
475 result in decreased susceptibility to both anti-gp41 components, which could explain the result.
476 Table 6 shows that viruses with resistance mutations targeted to both gp41 inhibitors do produce
477 an enhanced fold-change. These mutations in envelope are relatively rare within the LANL

database, with the Q577R mutation found in 1.9% of 5454 sequences (2017 release), while Q577K was found in only 8 isolates (0.15%). The L544V mutation was found in 2.8% of the isolates in the LANL.

The effect of connecting the 3 independent entry inhibitors together has several advantages compared to a mixture of individual inhibitors. An obvious advantage is the need to progress only one clinical candidate through the development pipeline rather than multiple separate molecules, although the added complexity of the macromolecule may make development more problematic. In addition, as observed when the two adnectins are joined or when the two anti-gp41 inhibitors are joined with the correct linkage, improved potency is achieved through multiple synergies. The improvement in potencies is the probable result of an avidity effect of placing the inhibitors near their site of action, driven by the binding of the anti-CD4 adnectin to its target. The peak synergy probably results from the greatly increased concentration of the two gp41 inhibitor components at the cell surface compared to the concentration if the gp41 inhibitors were floating in plasma. The higher local concentration of inhibitors should greatly increase their binding on-rate to gp41, and hence their potency, which is what was seen experimentally even when only the anti-gp41 adnectin was linked to an anti-CD4 adnectin (Table 4) (22). Studies on linker length connecting the two adnectins suggest that an optimal distance between the two inhibitors is needed, and if that distance is increased, the potency begins to decrease (22). Thus, GSK3732394 contains linker lengths and compositions that are optimal for the gp41 inhibitors to engage the 3-helix trimer and block it from converting to the 6-helix state. This is similar to the potency increase observed when certain bnAbs are linked in a heterologous mAb to ibalizumab (19).

500 Another advantage to linking the three inhibitors can be observed when the molecule is
501 tested against viruses containing mutations known to induce resistance to the various
502 components. Virus containing resistance mutations to one, two or all three inhibitor components
503 were recombinantly generated and examined against the individual inhibitors or GSK3732394
504 (Table 6). Against the individual inhibitors, significant fold changes compared to wild type virus
505 were observed as expected against the homologous virus/inhibitor pair. However, viruses
506 containing resistance mutations to only one of the inhibitors did not exhibit a significant fold
507 change (1.1-2.1 FC) against GSK3732394. This compares to >660-FC against the anti-gp41
508 adnectin or 7.0-FC against the peptide inhibitor. A significant fold change against a recombinant
509 virus is observed only if it contains resistance mutations to all 3 component inhibitors (98-FC) or
510 to the two anti-gp41inhibitors (89-FC) in the protein. This suggests that linking the inhibitors
511 into a single molecule should improve the resistance barrier compared to the individual
512 components, since a virus would need resistance to multiple inhibitors to see a phenotypic
513 change. A lack of a significant fold change is also observed in recombinant viruses with
514 resistance to the anti-CD4 adnectin and either of the two anti-gp41 inhibitors (Table 6).
515 Resistance to the anti-CD4 adnectin maps to loss of potential N-linked glycosylation sites in
516 gp120 and does not affect the binding of the adnectin to CD4 (28). Thus, even in these latter two
517 doubly resistant viruses, GSK3732394 is bound to CD4, although not producing an optimal
518 antiviral effect. Therefore, this strongly suggests that the high potency observed with
519 GSK3732394 is driven by the anti-gp41 inhibitors, while the synergy is driven by binding of the
520 molecule to CD4 through the action of the anti-CD4 adnectin.

521 This enhanced resistance barrier is further exemplified by the length of time it took to
522 select for a fully resistant virus in cell culture (Figure 5). It took approximately 6 months and 33

523 cell culture passages for virus with a significant fold change to be selected against GSK3732394.
524 Interestingly, initial changes were observed as early as passages 9-12, where one PNGS site was
525 lost and the key resistance mutation against the anti-gp41 adnectin (Q577R) appeared, although
526 the fold change was still low. Loss of PNGSs is the mechanism of resistance development to the
527 anti-CD4 adnectin, but it took the loss of multiple sites to induce resistance to the individual
528 adnectin (28). By passage 24, the Q577R mutation was fixed as well as additional mutations at
529 396/401, these mutations potentially affecting the occupancy of another PNGS between those
530 amino acids. An additional mutation of T138I was fixed at this time point and a mutation at T63I
531 was observed at ~30% frequency. The T63I change does not affect a PNGS, but the T138I
532 mutation does delete another PNGS in the envelope (perhaps reducing PGNSs by 3-4), which
533 could affect the susceptibility to the anti-CD4 adnectin. Interestingly, this virus still retained a
534 relatively low fold change. This is not surprising, as even if it has reduced susceptibility to both
535 adnectins, data from Table 6 shows that it should still be susceptible to GSK3732394. Peptide
536 resistance due to the L544S change is borne out in the next two sets of sequenced passages (33
537 and 37), where the increase in L544S to 50% and then 100% results in a large jump to 18.7- and
538 19.7-fold changes. At this point, the virus has selected mutations that reduce susceptibility to all
539 three inhibitors, and thus induce a significant, but not overly high fold change. This could
540 suggest that the synergistic potential of the combined molecule allows it to retain a fair amount
541 of activity even when resistance is developed against all individual components.

542 Perhaps the most advantageous property associated with GSK3732394 is its ability to
543 produce high potency at low levels of CD4 receptor occupancy (Figure 4). At the EC_{50} of
544 GSK3732394, only ~0.2% of CD4 on the cell surface is bound, while at the EC_{90} concentration,
545 only ~1.5% of CD4 is bound by inhibitor. How then is inhibitor bound to such a small

546 percentage of CD4 protein able to inhibit virus at an EC_{90} level? The increased local
547 concentration of the anti-gp41 inhibitors clearly helps, but the very high percentage (>>95%) of
548 free CD4 molecules on the cell still provides unencumbered target for virus to bind to, while any
549 virus bound to a CD4 protein also bound by GSK3732394 will be inhibited by the anti-CD4
550 adnectin. The most logical explanation is that GSK3732394 can inhibit *in trans* by having the
551 anti-gp41 inhibitors reach out and inhibit fusion of virus bound to a different CD4 molecule on
552 the cell. Based upon the antiviral and biophysical data obtained with GSK3732394, the
553 individual components and the partial progenitor constructs, a structural model to explain the
554 high degree of synergy can be proposed. The model takes into account what is known about the
555 stoichiometry of gp160 and the fusion process. For instance, electron microscopy studies show
556 that each HIV-1 virion contains between 7- 14 trimer spikes (39, 40). In addition, multiple trimer
557 spikes need to undergo a series of conformational changes to form the fusion pore, which
558 initiates virus-cell fusion. (40, 41). In the model, GSK3732394, when attached to CD4 via the
559 anti-CD4 adnectin domain, becomes anchored on the surface of the CD4+ T-cell at an optimal
560 distance from the cell surface to interact with the long lived 3-helix gp41 trimer spike bound to a
561 separate CD4 molecule (Figure 9).

562 The overall effect of the binding of GSK3732394 has a number of aspects. First, it
563 reduces the number of CD4 molecules on a T-cell available for functional attachment of the virus
564 and formation of the fusion pore. For instance, if one has ~50% receptor occupancy at trough,
565 this suggests that for most of the dosing period, more than half of the molecules on the cell are
566 engaged with GSK3732394, which may make it difficult to form a functional fusion pore with
567 multiple proteins if the anti-gp41 components work *in trans*. Second, the higher local
568 concentration of inhibitors should also greatly increase their effective binding on-rate to gp41,

569 and hence their potency. Studies on linker length connecting the two adnectins suggest that an
570 optimal distance between the two inhibitors is needed, and if that distance is increased, the
571 potency begins to decrease (22) Thus, GSK3732394 contains a linker length that is optimal for
572 the gp41 inhibitors to engage the 3-helix trimer and block it from converting to the 6-helix state,
573 and since the gp41 inhibitors probably work *in trans*, the mobility of the drug-bound CD4
574 molecules, and their ability to deliver the gp41 inhibitors to the sites of the fusion intermediates
575 during the brief window in which they are accessible, is likely a key to the mechanism of action.
576 The overall result is that inhibition by the complete GSK3732394 is much more potent than the
577 sum of its parts.

578 In order to probe its ability to inhibit virus infection *in vivo* as a long acting agent,
579 GSK3732394 was examined in a humanized mouse model of infection. Humanized mice were
580 infected with virus for 37 days and then treated every three days subcutaneously with either 4,
581 12.5 or 32 mg/kg of GSK3732394 for 63 days. The animals showed a dose dependent increase in
582 CD4 receptor occupancy and a dose dependent decrease in viral load, with 4/7 animals at the 32
583 mg/kg dose exhibiting viral titers below the level of detection by Day 63 of dosing.
584 GSK3732394 was effective at all 3 doses in a dose dependent fashion, with $\geq$1 $\log_{10}$ decrease in
585 viral titers after 9 days in the 12.5 and 32 mg/kg dose groups, with the 4 mg/kg dose group
586 decreasing viral titers 1 $\log_{10}$ by Day 27. Thus, GSK3732394 is effective as an antiviral agent *in*
587 *vivo*. The 32 mg/kg dose produced viral load decreases of >3 log10 by Day 27 and the profile
588 was similar to that seen when mice were treated with a daily regimen of RAL, 3TC and TDF. In
589 the 4 and 12.5 mg/kg dose groups, viral titers began to rebound between Days 36-45. Receptor
590 occupancies in the highest dose group were between 40-60% at trough, with lower ROs at the
591 lower doses. At Day 63, plasma from all but one mouse contained the single Q577R mutation

592 (the only change seen in any sample) reflective of resistance selection to the anti-gp41 adnectin.
593 Thus, Q577R was probably selected over the dosing term by GSK3732394. Although *in vitro* a
594 virus with a Q577R substitution should retain susceptibility to GSK3732394 (Table 6), the
595 potentially suboptimal concentrations of GSK3732394, illustrated by the receptor occupancies in
596 Figure 7, probably allows for this selection and virus breakthrough. One can envision a scenario
597 whereby at the lower ROs, occasionally there will be a situation where a GSK3732394-bound
598 CD4 is not close enough to a gp160 bound CD4 to allow for inhibition by the anti-gp41
599 components *in trans*, so the virus can infect the cell. Once infected, GSK3732394, as an entry
600 inhibitor, has no effect on the infected cell, which can produce new virions. From these and
601 resistance selection studies, it appears that the anti-gp41 adnectin has the lowest resistance
602 barrier of the 3 inhibitors, as it is the first mutation selected *in vivo*. Even, at the highest dose of
603 32 mg/kg, the RO of 40-60% may be enough to suppress some, but not all mice from selecting
604 Q577R. In this animal model, higher RO may be needed for GSK3732394 dosed as
605 monotherapy to completely suppress virus and avoid the selection of Q577R during longer term
606 treatment. All in all, these data describe a novel tri-specific inhibitor of HIV-1 virus-cell fusion
607 that has the potential to be a long acting inhibitor of virus infection. Although GSK3732394
608 could be used as a part of a long acting HAART regimen, achievement of high receptor
609 occupancy levels may allow it to be used as a standalone therapy under certain conditions. As
610 with all biologic proteins, a current unknown is the potential immunogenicity of the molecule
611 and the effect this might have on its potency and pharmacokinetic properties. Subcutaneously
612 dosed GSK3732394 has begun Phase 1 studies in order to answer these questions and to study its
613 potential as a long acting antiretroviral agent.

614

615

616 **Materials and Methods**

617 **Expression and purification of adnectin-peptide molecules.** Adnectins with different linkers
618 and/or peptides at the carboxy end of the anti-gp41adnectin were expressed with His tags at the
619 amino terminus of the adnectin and purified via cobalt affinity chromatography as described
620 (28).

621 **Expression and purification of GSK3732394.** GSK3732394 was expressed via transient
622 transfection of HEK293-6E cells. Briefly, HEK 293-6E cells were seeded into a 1-L shake flask
623 containing 350 mL of F17 medium (Invitrogen) supplemented with Glutamax (0.3 mM;
624 Invitrogen) and Pluronic F68 (0.1%; Invitrogen) at a density of $7x10^5$ cells/mL. Cells were
625 grown overnight at 37^oC, 5% CO_2, 80% humidity with shaking at 110 RPM. The following day,
626 cells were transfected with expression plasmid DNA using the Polyplus Transfection Reagent
627 PEIpro (VWR) according to the manufacturer's recommendations. The day after transfection,
628 cells were fed with 18 mL/flask of 20% Tryptone N1 (Fisher Scientific). Cells were cultured for
629 an additional 5 days. Harvest of conditioned medium was accomplished by centrifugation to
630 pellet cells.

631 GSK3732394 was purified using three chromatography steps followed by a final
632 ultrafiltration/diafiltration (UFDF) step for concentration and formulation. Initially, hydrophobic
633 interaction chromatography (HIC) purification was accomplished with a Toyopearl butyl 650M
634 column (Tosoh). The eluate was then subjected to additional chromatography using 40 μM type
635 I ceramic hydroxyapatite resin (BioRad). Anion-exchange chromatography using a Poros HQ50
636 column was employed as a final polishing step. The final eluate was concentrated to 10 mg/ml

using a Millipore Pellicon 2 50 Kd 0.1M^2 membrane and then buffer exchanged with 6 volumes of 25 mM phosphate, 150 mM trehalose, pH 6.8. Post concentration, the product was spiked to 0.1% pluronic F68 and sterile filtered.

Kinetics of binding to defined targets. Determination of the binding kinetics of the two individual adnectins has been described (22, 28). Binding activity of the peptide component was determined using His-tagged PRD-828 (Supplemental Table 2). This peptide contains three identical sequence segments from the HR1, and two segments from the HR2 regions of gp41, and spontaneously forms a five-helix bundle, displaying a single open peptide binding site, analogous to that described (42). By design, PRD-828 contains only the stretch of gp41 involved in peptide binding, and does not include the N17 region. Neutravidin (Pierce) was diluted to 10 μg/mL in 10 mM acetate, pH 4.5, and immobilized on a T-series CM5 Biacore chip (GE Healthcare) via a standard amine coupling kit (GE Healthcare) to a level of 6200 RU. The neutravidin surface was conditioned with three injections of 1 M NaCl, 40 mM NaOH. Biotinylated 5-helix bundle peptide PRD-828 was diluted in running buffer (HBS-P+; GE Healthcare) to 10 nM and flowed over the neutravidin surface until 122 RU had accumulated. GSK3732394 diluted in running buffer was flowed over the captured PRD-828 surface at 37°C at various concentrations at a flow rate of 50 μL/min with a contact time of 3 min. Dissociation was measured for 2 min or 10 min. A surface consisting of non-binding peptide biotin-IZIZ (Supplemental Table 2) captured onto neutravidin was used for reference subtraction, and buffer-only samples were included for background subtraction. The PRD-828 surface was regenerated between cycles with two injections of 0.1% SDS. A 1:1 Langmuir binding model was fit to the double-referenced sensorgrams to determine kinetic parameters using Biacore T100 Evaluation Software, version 2.0.1 (GE Healthcare).

Cells, viruses and antiviral assays. MT-2, HEK 293T, CEM-NKR-CCR5-Luc cells, the proviral DNA clone of NL_{4-3}, and primary clinical isolates were obtained from the NIH AIDS Research and Reference Reagent Program. B6 cells were also used and contain an integrated copy of a luciferase marker gene driven by the HIV-LTR (43). The replication competent NL_{4-3} variant RepRlucNL virus expresses *Renilla* luciferase and was used for most antiviral assays as described (44). Populations of envelope clones were obtained and used as described (28). Cytotoxicity was determined in MT-2 cells after 4 days incubation using XTT (2,3-bis-(2-methoxy-4-nitro-5-sulfophenyl)-2H-tetrazolium-5-carboxanilide) to measure cell viability using an established protocol (45).

Primary clinical isolates were examined for susceptibility to GSK3732394 using the CEM-NKR-CCR5-Luc cells as a reporter line. The human T-cell line, CEM-NKR-CCR5-Luc expresses CD4, CXCR4 and CCR5 receptors on its cell surface and carries the luciferase reporter gene under transcriptional control of the HIV-2 LTR. (46) For susceptibility analyses, the virus was used to infect CEM-NKR-CCR5-Luc cells in the presence or absence of serial dilutions of compound. On the assay set up day, $5x10^6$ cells were prepared per 96 well plate and were concentrated via low speed centrifugation at 1000 rpm and resuspended in 0.5 ml. HIV-1 viruses were incubated with the cells at $37^oC/5\%$ CO_2 for 1 hour within the range of MOI of 0.005 to 0.01. Serial four- or five-fold dilutions of GSK3732394 or other inhibitors were diluted in a 10 µl volume on a 96 well black/clear bottom plate. The cell-virus mix was diluted to the proper volume using assay media (RPMI 1640 supplemented with 10% heat inactivated fetal bovine serum (FBS), 100 units/ml penicillin /100 µg/ml streptomycin, 10 µg/ml polybrene) and 190 µl was added to each well culture plate. The cultures were incubated at 37°C/5%CO_2 for 5-8 days and the assay was processed and quantitated for virus growth by the amount of expressed

683 luciferase using the Bright-glo Luciferase kit (Promega). Susceptibility of viruses to inhibitors
684 were determined by XL-Fit analysis of luciferase signals. The results from 2 experiments were
685 averaged to establish the EC_{50} values.

686 **Resistance selection.** Two million MT-2 cells were infected with $NL_{4\text{-}3\ virus}$ in the presence of a
687 2X EC_{50} inhibitor concentration at an MOI of 0.005 to 0.05. Syncytium formation as a marker
688 for viral infection was monitored. When syncytium formation reached ~>10%, 1/1000 to 1/100
689 volume of the infectious supernatant was then transferred to fresh MT-2 cells in the presence of
690 the inhibitor at an increased concentration of 2X stepwise. When consistent virus breakthrough
691 was observed, the viral supernatant was evaluated against the inhibitor in the B6 antiviral assay.
692 a potency shift of more than 10-fold usually indicates the appearance of resistant virus. The
693 infected cells or the viral supernatants were used to obtain the viral genomes by PCR or RT-
694 PCR, followed by sequencing to identify the amino acid changes. Amino acid changes were then
695 introduced to viral genome using site-directed mutagenesis and cloning. The recombinant viruses
696 were evaluated in a replicating virus assay for potency shift vs. wild type virus.

697 **Mouse model and efficacy studies.** GSK3732394 was examined for efficacy in a humanized
698 mouse model of HIV infection established and running at TransCure bioServices SAS
699 (Archamps, France). NOD/Shi-scid/IL-2Rγnon-specific immunodeficient mouse strain (NOG)
700 was humanized with hematopoietic stem cells isolated from cord blood. After reconstitution of
701 the human immune system and confirmation of the presence of CD4+ cells (about 14 weeks
702 post-transplant), the hu-mice were infected with HIV-1 YU2 strain. A total of 40 mice with
703 >25% of circulating human CD45+ were used in the study. Selected hu-mice were inoculated
704 with the HIV YU2 strain by intra-peritoneal injection. Infection proceeded for 31 days after
705 which plasma was obtained to assess viral loads by qRT-PCR and the level of human CD4+ cells

706 by flow cytometry. Mice were placed into 5 groups, normalizing HIV viral loads and human
707 CD4 cells across the different groups. There were 3 groups treated with GSK37323794; 4, 12.5
708 and 32 mg/kg, along with a vehicle treatment group and a control HAART treated group given
709 raltegravir, lamivudine and tenofovir disproxil fumarate in their food. The GSK3732394 and
710 vehicle treatment groups were dosed SC starting on Day 37 post infection every 3 days, while
711 the HAART treatment group was dosed daily in food. Dosing continued for an additional 60
712 days (20 doses). At every third dose (9 days) during the dosing schedule, plasma was obtained
713 prior to the SC injection for analysis of viral loads and receptor occupancy. At Day 63 post-
714 dosing (Day 100 post virus infection), most mice were sacrificed, except for 3 mice in the
715 HAART treated group and 3 mice in the 32 mg/kg dosed group. Those mice were kept for an
716 additional 21 days without drug treatment to look at virus rebound. Plasma was obtained from
717 these animals after 9 days and at the end of the experiment.

718 Viral loads were determined using 20µl of extracted plasma. HIV loads were determined
719 using the "Generic HIV Charge Virale" quantitation kit (Biocentric, France). HIV loads were
720 considered not detectable when Ct values were lower than 37. Limit of sensitivity was estimated
721 to be 500 copies/ml. Receptor occupancy of GSK3732394 was determined via flow cytometry on
722 an Attune NxT Flow Cytometer (Life Technologies). Human immune hematopoietic sub-
723 populations were monitored using FITC anti-human CD3 (Miltenyi Biotec), anti-CD4 mAb
724 OKT4 (BioLegend), Brilliant Violet 510 anti-human CD8 (BD Biosciences) and an AlexaFluor
725 647 labeled anti-CD4 adnectin, 4945_G06-107 (28).

726 Receptor occupancy of GSK3732394 was determined via flow cytometry on an Attune
727 NxT Flow Cytometer (Life Technologies). OKT4 does not compete with GSK3732394 for
728 binding to CD4, and therefore can be used as a marker for CD4+ cells regardless of the presence

729 of GSK3732394. The AF647-4945_G06 adnectin does compete with GSK3732394 for binding
730 to CD4, and is used as a probe for occupancy. For each timepoint, the AF647 median
731 fluorescence intensity (MFI) of the CD4+/CD8-/CD3+ cell population from vehicle control
732 animals was indicative of 0% occupancy, and the AF647 MFI of the CD4-/CD8+/CD3+
733 population from GSK3732394-dosed animals was used as a surrogate for 100% occupancy. The
734 % RO for a given sample was then calculated using this equation:

$$\%RO = 100 * (1 - \frac{Sample\ AF647\ MFI_{CD4+CD8-CD3+} - Sample\ AF647\ MFI_{CD4-CD8+CD3+}}{Vehicle\ AF647\ MFI_{CD4+CD8-CD3+}})$$

735 Plasma levels of GSK3732394 were quantitated via an ELISA assay. Streptavidin-coated
736 black 96-well plates were coated with biotinylated PRD-828 at 1 ug/ml in PBST (Invitrogen) for
737 1 hour at room temperature. The coated plates were washed 3 times with PBST and then
738 incubated with SuperBlocker T20 (Thermo Scientific) blocking buffer for 1 hour. The plates were
739 washed 3 times with PBST and mouse plasma samples were serially diluted 5-fold and added to
740 the assay ready plate. The plates were incubated at room temperature with shaking for 1 hour and
741 washed 3 times with PBST before 1:20000 diluted Goat pAb anti HSA-HRP antibody (AbCam)
742 was applied for 30 minutes. Plates were washed 3 times with PBST and developed with
743 Supersignal ELISA pico substrate (Thermo Scientific). Signals were read on an EnVision plate
744 reader. Concentrations were determined through comparison with a standard curve, which was
745 created through 3-fold dilutions of GSK3732394 in PBST with added normal mouse plasma
746 (VWR).

747 For PCR amplification of gp160 genes in mouse plasma, HIV-1 viral RNA was
748 extracted from 200 µl of mice plasma samples using a QIAamp MinElutevirus kit and eluted
749 in 40 µl of RNase-free water. cDNA was generated from 34 µl viral RNA using SuperScript
750 III first strand synthesis kit (Invitrogen) per the manufacturer's protocol. Eighty µl of cDNA

solution was run over the MinElute PCR Purification Kit (Qiagen) and eluted in 10 µl of EB buffer per manufacturer's protocol. Amplification used YU2 specific primers outside of the envelope gene using the Platinum Taq polymerase High Fidelity kit (Invitrogen) The first-round PCR product was purified using a MinElutePCR Purification Kit, eluted in 10 µl of EB buffer and used as template for the second round of PCR. Amplified envelope PCR products were subjected to population-based sequencing using a library of envelope-specific primers. The HIV-1 env sequences from the mice were aligned to the YU2 sequence obtained from TransCure using AlignX software in the Vector NTI package (Invitrogen).

Acknowledgments

The authors would like to acknowledge Mei Sun, Yulia Benitez, Dieter Drexler and many other present and former employees of Bristol-Myers Squibb for their support of this program. ViiV Healthcare has assumed responsibility for clinical development of GSK3732394.

Most authors were employees of Bristol-Myers Squibb at the time of this work and many of those are currently employed by ViiV Healthcare.

References

1. Corado KC, Caplan MR, Daar ES. 2018. Two-drug regimens for treatment of naive HIV-1 infection and as maintenance therapy. Drug Des Devel Ther 12:3731-3740.
2. Kelly SG, Nyaku AN, Taiwo BO. 2016. Two-Drug Treatment Approaches in HIV: Finally Getting Somewhere? Drugs 76:523-31.
3. Margolis DA, Gonzalez-Garcia J, Stellbrink HJ, Eron JJ, Yazdanpanah Y, Podzamczer D, Lutz T, Angel JB, Richmond GJ, Clotet B, Gutierrez F, Sloan L, Clair MS, Murray M, Ford SL, Mrus J, Patel P, Crauwels H, Griffith SK, Sutton KC, Dorey D, Smith KY, Williams PE, Spreen WR. 2017. Long-acting intramuscular cabotegravir and rilpivirine in adults with HIV-1 infection (LATTE-2): 96-week results of a randomised, open-label, phase 2b, non-inferiority trial. Lancet 390:1499-1510.
4. Spreen W, Williams P, Margolis D, Ford SL, Crauwels H, Lou Y, Gould E, Stevens M, Piscitelli S. 2014. Pharmacokinetics, safety, and tolerability with repeat doses of GSK1265744 and rilpivirine (TMC278) long-acting nanosuspensions in healthy adults. J Acquir Immune Defic Syndr 67:487-92.
5. Kerrigan D, Mantsios A, Gorgolas M, Montes ML, Pulido F, Brinson C, deVente J, Richmond GJ, Beckham SW, Hammond P, Margolis D, Murray M. 2018. Experiences with long acting injectable ART: A qualitative study among PLHIV participating in a Phase II study of cabotegravir + rilpivirine (LATTE-2) in the United States and Spain. PLoS One 13:e0190487.
6. Beccari MV, Mogle BT, Sidman EF, Mastro KA, Asiago-Reddy E, Kufel WD. 2019. Ibalizumab: A novel monoclonal antibody for the management of multidrug resistant HIV-1 infection. Antimicrob Agents Chemother doi:10.1128/AAC.00110-19.
7. Dhody K, Pourhassan N, Kazempour K, Green D, Badri S, Mekonnen H, Burger D, Maddon PJ. 2018. PRO 140, a monoclonal antibody targeting CCR5, as a long-acting, single-agent maintenance therapy for HIV-1 infection. HIV Clin Trials 19:85-93.
8. Sok D, Burton DR. 2019. Publisher Correction: Recent progress in broadly neutralizing antibodies to HIV. Nat Immunol 20:374.
9. Sok D, Burton DR. 2018. Recent progress in broadly neutralizing antibodies to HIV. Nat Immunol 19:1179-1188.
10. Wagh K, Seaman MS, Zingg M, Fitzsimons T, Barouch DH, Burton DR, Connors M, Ho DD, Mascola JR, Nussenzweig MC, Ravetch J, Gautam R, Martin MA, Montefiori DC, Korber B. 2018. Potential of conventional & bispecific broadly neutralizing antibodies for prevention of HIV-1 subtype A, C & D infections. PLoS Pathog 14:e1006860.
11. Bar-On Y, Gruell H, Schoofs T, Pai JA, Nogueira L, Butler AL, Millard K, Lehmann C, Suarez I, Oliveira TY, Karagounis T, Cohen YZ, Wyen C, Scholten S, Handl L, Belblidia S, Dizon JP, Vehreschild JJ, Witmer-Pack M, Shimeliovich I, Jain K, Fiddike K, Seaton KE, Yates NL, Horowitz J, Gulick RM, Pfeifer N, Tomaras GD, Seaman MS, Fatkenheuer G, Caskey M, Klein F, Nussenzweig MC. 2018. Safety and antiviral activity of combination HIV-1 broadly neutralizing antibodies in viremic individuals. Nat Med 24:1701-1707.
12. Caskey M, Klein F, Nussenzweig MC. 2019. Broadly neutralizing anti-HIV-1 monoclonal antibodies in the clinic. Nat Med doi:10.1038/s41591-019-0412-8.

13. Steinhardt JJ, Guenaga J, Turner HL, McKee K, Louder MK, O'Dell S, Chiang CI, Lei L, Galkin A, Andrianov AK, N AD-R, Bailer RT, Ward AB, Mascola JR, Li Y. 2018. Rational design of a trispecific antibody targeting the HIV-1 Env with elevated anti-viral activity. Nat Commun 9:877.
14. Khan SN, Sok D, Tran K, Movsesyan A, Dubrovskaya V, Burton DR, Wyatt RT. 2018. Targeting the HIV-1 Spike and Coreceptor with Bi- and Trispecific Antibodies for Single-Component Broad Inhibition of Entry. J Virol 92.
15. Padte NN, Yu J, Huang Y, Ho DD. 2018. Engineering multi-specific antibodies against HIV-1. Retrovirology 15:60.
16. Augusto MT, Hollmann A, Castanho MA, Porotto M, Pessi A, Santos NC. 2014. Improvement of HIV fusion inhibitor C34 efficacy by membrane anchoring and enhanced exposure. J Antimicrob Chemother 69:1286-97.
17. Ingallinella P, Bianchi E, Ladwa NA, Wang YJ, Hrin R, Veneziano M, Bonelli F, Ketas TJ, Moore JP, Miller MD, Pessi A. 2009. Addition of a cholesterol group to an HIV-1 peptide fusion inhibitor dramatically increases its antiviral potency. Proc Natl Acad Sci U S A 106:5801-6.
18. Song R, Pace C, Seaman MS, Fang Q, Sun M, Andrews CD, Wu A, Padte NN, Ho DD. 2016. Distinct HIV-1 Neutralization Potency Profiles of Ibalizumab-Based Bispecific Antibodies. J Acquir Immune Defic Syndr 73:365-373.
19. Pace CS, Song R, Ochsenbauer C, Andrews CD, Franco D, Yu J, Oren DA, Seaman MS, Ho DD. 2013. Bispecific antibodies directed to CD4 domain 2 and HIV envelope exhibit exceptional breadth and picomolar potency against HIV-1. Proc Natl Acad Sci U S A 110:13540-5.
20. Fetzer I, Gardner MR, Davis-Gardner ME, Prasad NR, Alfant B, Weber JA, Farzan M. 2018. eCD4-Ig Variants That More Potently Neutralize HIV-1. J Virol 92.
21. Fellinger CH, Gardner MR, Weber JA, Alfant B, Zhou AS, Farzan M. 2019. eCD4-Ig limits HIV-1 escape more effectively than CD4-Ig or a broadly neutralizing antibody. J Virol doi:10.1128/JVI.00443-19.
22. Wensel D, Sun Y, Davis J, Li Z, Zhang S, McDonagh T, Fabrizio D, Cockett M, Krystal M. 2018. A Novel gp41-Binding Adnectin with Potent Anti-HIV Activity Is Highly Synergistic when Linked to a CD4-Binding Adnectin. J Virol 92.
23. Lipovsek D. 2011. Adnectins: engineered target-binding protein therapeutics. Protein Eng Des Sel 24:3-9.
24. Sachdev E, Gong J, Rimel B, Mita M. 2015. Adnectin-targeted inhibitors: rationale and results. Curr Oncol Rep 17:35.
25. Koide A, Bailey CW, Huang X, Koide S. 1998. The fibronectin type III domain as a scaffold for novel binding proteins. J Mol Biol 284:1141-51.
26. Koide S, Koide A, Lipovsek D. 2012. Target-binding proteins based on the 10th human fibronectin type III domain ((1)(0)Fn3). Methods Enzymol 503:135-56.
27. Tolcher AW, Sweeney CJ, Papadopoulos K, Patnaik A, Chiorean EG, Mita AC, Sankhala K, Furfine E, Gokemeijer J, Iacono L, Eaton C, Silver BA, Mita M. 2011. Phase I and pharmacokinetic study of CT-322 (BMS-844203), a targeted Adnectin inhibitor of VEGFR-2 based on a domain of human fibronectin. Clin Cancer Res 17:363-71.
28. Wensel D, Sun Y, Li Z, Zhang S, Picarillo C, McDonagh T, Fabrizio D, Cockett M, Krystal M, Davis J. 2017. Discovery and Characterization of a Novel CD4-Binding Adnectin with Potent Anti-HIV Activity. Antimicrob Agents Chemother 61.

29. Yi HA, Fochtman BC, Rizzo RC, Jacobs A. 2016. Inhibition of HIV Entry by Targeting the Envelope Transmembrane Subunit gp41. Curr HIV Res 14:283-94.
30. Dwyer JJ, Wilson KL, Davison DK, Freel SA, Seedorff JE, Wring SA, Tvermoes NA, Matthews TJ, Greenberg ML, Delmedico MK. 2007. Design of helical, oligomeric HIV-1 fusion inhibitor peptides with potent activity against enfuvirtide-resistant virus. Proc Natl Acad Sci U S A 104:12772-7.
31. Huerta-Garcia G, Chavez-Garcia M, Mata-Marin JA, Sandoval-Ramirez J, Dominguez-Hermosillo J, Rincon-Rodriguez AL, Gaytan-Martinez J. 2014. Effectiveness of enfuvirtide in a cohort of highly antiretroviral-experienced HIV-1-infected patients in Mexico. AIDS Res Ther 11:323.
32. Seay K, Qi X, Zheng JH, Zhang C, Chen K, Dutta M, Deneroff K, Ochsenbauer C, Kappes JC, Littman DR, Goldstein H. 2013. Mice transgenic for CD4-specific human CD4, CCR5 and cyclin T1 expression: a new model for investigating HIV-1 transmission and treatment efficacy. PLoS One 8:e63537.
33. Yu F, Lu L, Du L, Zhu X, Debnath AK, Jiang S. 2013. Approaches for identification of HIV-1 entry inhibitors targeting gp41 pocket. Viruses 5:127-49.
34. Poveda E, Briz V, Soriano V. 2005. Enfuvirtide, the first fusion inhibitor to treat HIV infection. AIDS Rev 7:139-47.
35. Kontermann RE. 2009. Strategies to extend plasma half-lives of recombinant antibodies. BioDrugs 23:93-109.
36. Song R, Oren DA, Franco D, Seaman MS, Ho DD. 2013. Strategic addition of an N-linked glycan to a monoclonal antibody improves its HIV-1-neutralizing activity. Nat Biotechnol 31:1047-52.
37. Manfroi B, McKee T, Mayol JF, Tabruyn S, Moret S, Villiers C, Righini C, Dyer M, Callanan M, Schneider P, Tzankov A, Matthes T, Sturm N, Huard B. 2017. CXCL-8/IL8 Produced by Diffuse Large B-cell Lymphomas Recruits Neutrophils Expressing a Proliferation-Inducing Ligand APRIL. Cancer Res 77:1097-1107.
38. Lin JH. 2009. Pharmacokinetics of biotech drugs: peptides, proteins and monoclonal antibodies. Curr Drug Metab 10:661-91.
39. Chertova E, Bess JW, Jr., Crise BJ, Sowder IR, Schaden TM, Hilburn JM, Hoxie JA, Benveniste RE, Lifson JD, Henderson LE, Arthur LO. 2002. Envelope glycoprotein incorporation, not shedding of surface envelope glycoprotein (gp120/SU), Is the primary determinant of SU content of purified human immunodeficiency virus type 1 and simian immunodeficiency virus. J Virol 76:5315-25.
40. Zhu P, Chertova E, Bess J, Jr., Lifson JD, Arthur LO, Liu J, Taylor KA, Roux KH. 2003. Electron tomography analysis of envelope glycoprotein trimers on HIV and simian immunodeficiency virus virions. Proc Natl Acad Sci U S A 100:15812-7.
41. Brandenberg OF, Magnus C, Rusert P, Regoes RR, Trkola A. 2015. Different infectivity of HIV-1 strains is linked to number of envelope trimers required for entry. PLoS Pathog 11:e1004595.
42. Root MJ. 2001. Protein Design of an HIV-1 Entry Inhibitor. Science 291:884-888.
43. Nowicka-Sans B, Gong YF, McAuliffe B, Dicker I, Ho HT, Zhou N, Eggers B, Lin PF, Ray N, Wind-Rotolo M, Zhu L, Majumdar A, Stock D, Lataillade M, Hanna GJ, Matiskella JD, Ueda Y, Wang T, Kadow JF, Meanwell NA, Krystal M. 2012. In vitro antiviral characteristics of HIV-1 attachment inhibitor BMS-626529, the active component of the prodrug BMS-663068. Antimicrob Agents Chemother 56:3498-507.

44. Li Z, Terry B, Olds W, Protack T, Deminie C, Minassian B, Nowicka-Sans B, Sun Y, Dicker I, Hwang C, Lataillade M, Hanna GJ, Krystal M. 2013. In vitro cross-resistance profile of nucleoside reverse transcriptase inhibitor (NRTI) BMS-986001 against known NRTI resistance mutations. Antimicrob Agents Chemother 57:5500-8.

45. Weislow OS, Kiser R, Fine DL, Bader J, Shoemaker RH, Boyd MR. 1989. New soluble-formazan assay for HIV-1 cytopathic effects: application to high-flux screening of synthetic and natural products for AIDS-antiviral activity. J Natl Cancer Inst 81:577-86.

46. Spenlehauer C, Gordon CA, Trkola A, Moore JP. 2001. A luciferase-reporter gene-expressing T-cell line facilitates neutralization and drug-sensitivity assays that use either R5 or X4 strains of human immunodeficiency virus type 1. Virology 280:292-300.

FIGURE LEGENDS

FIGURE 1 Effect of joining the peptide inhibitor to the carboxy terminus of the anti-gp41 adnectin. Potencies of individual fusion peptide inhibitors fused to an inactive adnectin were compared to potencies of the same peptides linked to an anti-gp41 adnectin (4773_A08) (22). The names of each protein are shown above the diagram and the sequences of each of the anti-fusion peptides are shown below the figure.

FIGURE 2 Potency of peptides with single amino acid substitutions of the Asp. The short peptide in the PRD-1022 adnectin-peptide fusion was mutated to replace the Asp (SRIEALIRAAQEQQEKNEAALRELDKWAS) residue with one of 15 other amino acids and examined for antiviral activity. Absolute EC_{50}s for each adnectin-peptide proteins are shown.

FIGURE 3 Amino acid sequence of GSK3732394/BMS-986197. The human serum albumin component is highlighted in red, the anti-CD4 and anti-gp41 adnectins are highlighted in green and blue, respectively, and the peptide is highlighted in purple. The linker sequences are not highlighted. In addition, the human serum albumin component contains a C34A mutation to remove the only free sulfhydryl group in the molecule.

FIGURE 4 Comparison of binding affinity of GSK3732394 to MT-2 cells with antiviral activity observed against RepRLucNL virus. Concentration of GSK3732394 is platted against% maximal activity (binding to CD4 or antiviral activity). The antiviral activity of the anti-CD4 adnectin alone superimposes with its cell binding activity, while the antiviral activity dose response of GSK3732394 is much stronger than that of its cell binding activity.

939 **FIGURE 5 Selection of GSK3732394-resistant virus.** Table at the top lists all the changes
940 observed during selection by passage 37 and the fold change compared to wild type NL_{4-3} virus.
941 Recombinant virus represents a pure RepRlucNL virus containing all the changes shown. For the
942 selection, population sequencing and susceptibility analysis of virus were performed every 3
943 passages (p) and are graphed as fold change (FC) versus wild type virus. GSK3732394
944 concentrations are shown on the right. Identified mutations are listed at specific passages in the
945 boxes, with estimated frequencies. If no frequency is listed, mutation was fixed at ~100%.

946 **FIGURE 6 Observed fold change of cloned envelope populations against GSK3732394 in a**
947 **cell-cell fusion assay.** Envelope populations were divided into subtypes as shown above.
948 Subtypes with one or a few envelopes are grouped into Others and the numbers of isolates and
949 color codes are shown to the right. Significant changes in susceptibility were estimated to be 10-
950 FC or above, as described in text.

951 **FIGURE 7** A) CD4 receptor occupancy with GSK3732394 in the YU2 infected humanized mice
952 and B) GSK3732394 concentrations at trough on the respective days of the study. The doses are
953 indicated by line type and the key is in the figure. Days denote time after first dose (not including
954 the 37 days of YU2 infection prior to firt dose).

955 **FIGURE 8 Efficacy of GSK3732394 in a mouse model of infection.** Lines represent viral titers in
956 dose cohorts, the identities of which are shown on the right. The numbers in fractions indicate the
957 number of samples with undetectable viral load at this time point. Since the lower limit of
958 quantitation of the QPCR assay was 100 copies/ml, for graphing purposed, undetectable
959 samples were arbitrarily given a viral load of 100 copies/ml.

960 **FIGURE 9 Model of inhibition by GSK3732394.** The CD4 molecule (A) is bound to the anti-
961 CD4 component of GSK3732394 (B and C). D) A gp41 molecule in the semi-stable 3-helix

962 conformation, as part of a gp160 trimer bound to a different CD4 within the fusion pore. The
963 GSK3732394 – CD4 complex is in the correct orientation and at an optimal distance for the anti-
964 gp41 adnectin and peptide inhibitors to allow them to bind to the gp41 (E), thus disarming 2
965 distinct epitopes on gp41. Color coding for the 3-hHIV-1 gp41: N-terminal fusion peptide
966 domain (teal), helical domain binding to peptide inhibitor (purple), N-terminal "N17" region
967 (green) and C-terminal domain (dark blue).

968

TABLE 1 Antiviral potency and binding affinity of peptide 203613-24

Assessment	Number of replicates		EC_{50} (nM)	EC_{90} (nM)
Antiviral activity[a]	21		0.40 ± 0.27	5.19 ± 3.53
		k_a (1/Ms)	k_d (1/s)	K_D (nM)
Target binding activity[b]	3	$4.3 \pm 1.7 \times 10^{6}$	$2.4 \pm 0.1 \times 10^{-4}$	0.06 ± 0.03

[a]Tested against RepRlucNL virus
[b]Kinetic measurements performed using the PRD-828 target

TABLE 2 Activity of 203613-24 against envelope proteins in the RepRlucNL with enfuvirtide resistance mutations

	Potency Fold-Change for Given Variant Relative to LAI Envelope[a]				
Inhibitor	G547D[b] (G36D)	V549A (V38A)	Q551H (Q40H)	N553T (N42T)	N554D (N43D)
Enfuvirtide	36.4 ± 8.3	167 ± 20	5.7 ± 4.7	9.3 ± 2.7	157 ± 157
203613-24	1.0 ± 0.6	17.7 ± 7.4	2.4 ± 1.5	2.3 ± 2.3	1.1 ± 0.1

[a]Fold change compared to LAI control envelope in a cell-cell fusion assay
[b]Mutation numbering based upon HXB2 sequence starting from gp120 or (gp41)

TABLE 3 Optimization of the linker between the anti-gp41 Adnectin and peptide[a]

Name	EC_{50} (nM)	C-terminal sequence of anti-N17 adnectin	Linker sequence
PRD-2767	4.8	NYRTEIE	GGGGSGGGGSGGGGSGGGG
PRD-2768	3.0	NYRTEIE	GGGGSGGGGSGGGG
PRD-2769	12.7	NYRTEIE	GGGGSGGGGSG
PRD-2770	10.3	NYRTEIE	GGGGSGGGG
PRD-2771	3.5	NYRTEIE	GGGGSG
PRD-2772	1.0	NYRTEIE	GGGGSGGGGSGGGGSGGGGSGGGG
PRD-2773	3.6	NYRTEIE	GGGGSGGGGSGGGGSGGGG
PRD-2774	2.1	NYRTEI	GGGGSGGGGSGGGGSGGGG
PRD-2775	1.2	NYRTE	GGGGSGGGGSGGGGSGGGG
PRD-2776	1.2	NYRTP	GGGGSGGGGSGGGGSGGGG

[a]All constructs contained the same peptide fusion inhibitor sequence (SEYEARIEALIRAAQEQQEKNEAALRELDK) C-terminal to the linker except for PRD-2773, which has Ala substituted for the Ser at the amino terminus of the peptide.

Note: This table is also provided as a separate TIF file (graphic file) due to the diagram graphics it contains

TABLE 4 Synergistic and antagonistic properties of joining the anti-HIV-1 adnectins and peptide

Designation	Diagram	EC_{50} (nM)[b]	Description
C		11.4 ± 4.4	anti-CD4 adnectin only
41		6.1 ± 0.1	anti-gp41 adnectin only
P		0.53 ± 0.16	peptide only
X[a]		>1000	inert adnectin only
C_X_		64.3 ± 18.1	anti-CD4 adnectin_inert adnectin_linker
X_41_		132.1 ± 9.8	inert adnectin_ anti-gp41adnectin_linker
X_41_P		61.7 ± 14.8	inert adnectin_ anti-gp41 adnectin_peptide
C_41		0.02 ± 0.01	anti-CD4 adnectin _ anti-gp41 adnectin
C_X_P		0.21 ± 0.03	anti-CD4 adnectin_inert adnectin_peptide
C_41_P		0.09 ± 0.01	anti-CD4 adnectin_ anti-gp41 adnectin_peptide
C+41+P	+ +	0.53 ± 0.02	1:1:1 mixture of the 3 individual inhibitors
GSK3732394	HSA-	0.27 ± 0.17	HSA_anti-CD4 adnectin_ anti-gp41 adnectin_peptide

[a]X = non-HIV-1 specific adnectin
[b]potency against RepRlucNL virus; average of 3 independent experiments

TABLE 5 Binding affinity of GSK3732394 to inhibitor targets and comparison to the individual inhibitors

Protein	Target	k_a (1/Ms)	k_d (1/s)	K_D (nM)
GSK3732394	Human CD4	$1.3 \pm 0.5 \times 10^{4}$	$7.5 \pm 0.7 \times 10^{-4}$	66 ± 38
6940_B01	Human CD4	$2.0 \pm 0.3 \times 10^{5}$	$7.5 \pm 0.5 \times 10^{-4}$	3.9 ± 0.7
GSK3732394	IZN24[a]	$9.1 \pm 3.5 \times 10^{5}$	$2.2 \pm 1.0 \times 10^{-3}$	2.4 ± 0.3
6200_A08	IZN24	$4.8 \pm 1.9 \times 10^{6}$	$3.5 \pm 0.5 \times 10^{-3}$	0.8 ± 0.4
GSK3732394	PRD-828	$7.1 \pm 2.2 \times 10^{5}$	$2.7 \pm 0.8 \times 10^{-4}$	0.4 ± 0.2
203613-24	PRD-828	$4.3 \pm 1.7 \times 10^{6}$	$2.4 \pm 0.1 \times 10^{-4}$	0.06 ± 0.03

[a]Target described in (22)

TABLE 6 Activity of GSK3732394, individual inhibitors, and C_41_P against RepRlucNL viruses with selected mutations that encode resistance to one or multiple components

Inhibitor	Anti-CD4^{Ra}	Anti-gp41^{R} Q577R	pep^{R} L544S	pep^{R} V549A	Anti-gp41^{R}/pep^{R} Q577R+ V549A	Anti-CD4^{R}+ Anti-gp41^{R}+ pep^{Rb}	Anti-CD4^{R}+ pep^{R}	Anti-CD4^{R}+ gp41^{R}
6940_B01	6.8^{c}	0.1	1.2	nd	0.8	3.2	nd	nd
6200_A08	0.4	>660	1.8	nd	>799.8	>660	nd	nd
203613-24	0.4	1.4	7.0	24.2	83.1	39.9	nd	nd
GSK3732394	1.1	1.9	2.1	6.8	89.1	98.0	nd	nd
C_41_P^{d}	0.5	3.7	1.3	nd	125	nd	0.3	0.4

^{a}Anti-CD4^{R} amino acid changes = S143R, N197D, N301K, and S465P
^{b}Virus contains the anti-CD4^{R} mutations + Q577R +V549A
^{c}Fold-change in EC_{50} compared to wild type ReprRlucNL
^{d}Performed in independent experiments
nd: Not done

TABLE 7 Activity of GSK3732394 against clinical isolates

Virus	Subtype	EC_{50} (nM)
92BR018	B	0.71
92BR028	B	1.95
10215-6	C	0.11
97ZA012	C	0.24
93RW034	A	0.70
94UG103	A	0.40
92UG046	D	0.42
92US660	B	0.26
92HT599	B	0.10
JEW	B	0.11
92UG029	A	0.05
98TZ017	C	0.06
94UG114	D	0.20
92TH001	CRF01_AE	0.19
RU570	G	1.07
91US056	B	0.07
93BR020	F	0.11
98BR004	C	0.23
92BR014	B	0.26
YBF30	Group N	0.85
BCF03	Group O	2.10

TABLE 8 Activity of inhibitors against YU2 virus

Inhibitor	Avg EC_{50} (nM)
6940_B01 (anti-CD4 adnectin)	90
6200_A08 (anti-gp41 adnectin)	238
203613-24 (peptide inhibitor)	136
GSK3732394	1.2

	Individual Adnectin	Adn + Short	Adn + Medium	Adn + Long
		5598_B01	**5626_E10**	**5586_A01**
	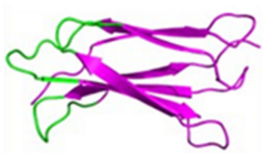			
EC_{50} (nM):	Inactive	>200	141	3.2
	4773_A08	**5626_A01**	**5626_E09**	**5626_A10**
	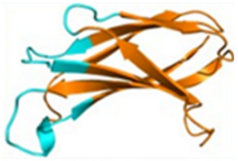		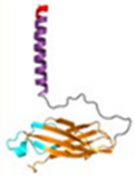	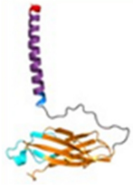
EC_{50} (nM):	48	4.8	0.7	1.1

Peptide	Sequence
Short	AEYEARIEALIRAAQEQQEKNEAALRELDK
Medium	TIAEYAARIEALIRAAQEQQEKNEAALRELDK
Long	TTWDRAIAEYAARIEALIRAAQEQQEKNEAALRELDK

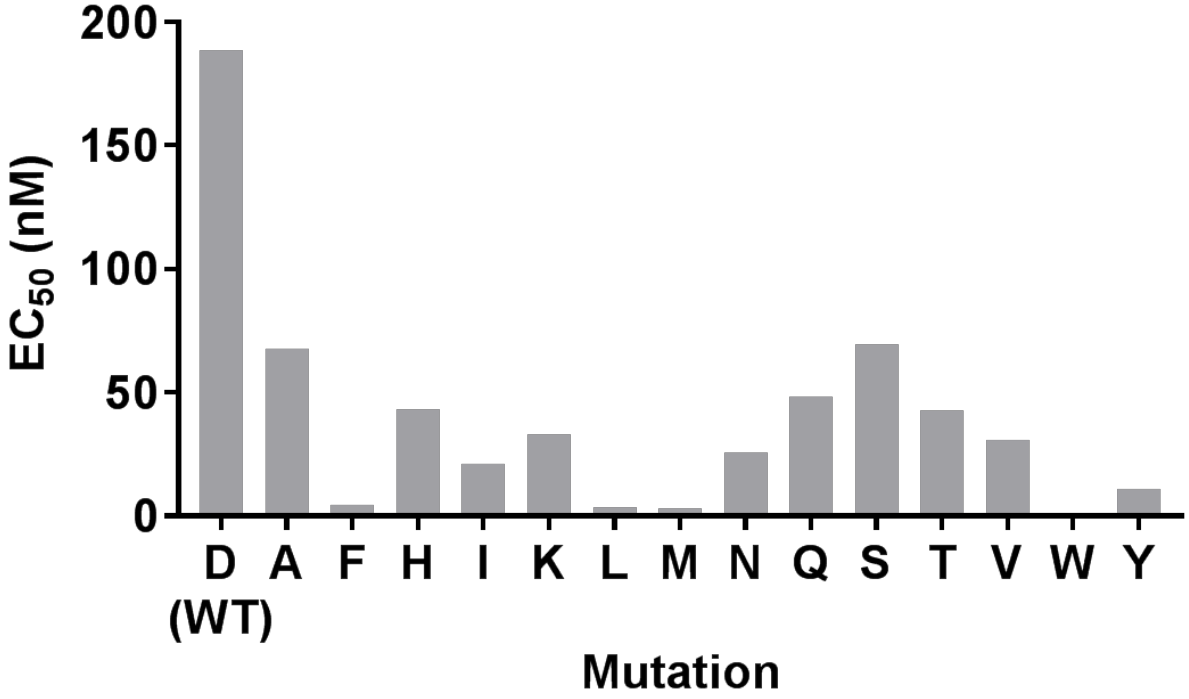

```
001 DAHKSEVAHR FKDLGEENFK ALVLIAFAQY LQQAPFEDHV KLVNEVTEFA KTCVADESAE 060
061 NCDKSLHTLF GDKLCTVATL RETYGEMADC CAKQEPERNE CFLQHKDDNP NLPRLVRPEV 120
121 DVMCTAFHDN EETFLKKYLY EIARRHPYFY APELLFFAKR YKAAFTECCQ AADKAACLLP 180
181 KLDELRDEGK ASSAKQRLKC ASLQKFGERA FKAWAVARLS QRFPKAEFAE VSKLVTDLTK 240
241 VHTECCHGDL LECADDRADL AKYICENQDS ISSKLKECCE KPLLEKSHCI AEVENDEMPA 300
301 DLPSLAADFV ESKDVCKNYA EAKDVFLGMF LYEYARRHPD YSVVLLLRLA KTYETTLEKC 360
361 CAAADPHECY AKVFDEFKPL VEEPQNLIKQ NCELFEQLGE YKFQNALLVR YTKKVPQVST 420
421 PTLVEVSRNL GKVGSKCCKH PEAKRMPCAE DYLSVVLNQL CVLHEKTPVS DRVTKCCTES 480
481 LVNRRPCFSA LEVDETYVPK EFNAETFTFH ADICTLSEKE RQIKKQTALV ELVKHKPKAT 540
541 KEQLKAVMDD FAAFVEKCCK ADDKETCFAE EGKKLVAASQ AALGLGGGGS GGGGSGGGGS 600
601 GGGGSGGGGS GVSDVPRDLE VVAATPTSLL ISWDAPAVTV HSYHIQYWPL GSYQRYQVFS 660
661 VPGSKSTATI SGLKPGVEYQ IRVYAETGGA DSDQSFGWIQ IGYRTPESPE PETPEDEGVS 720
721 DVPRDLEVVA ATPTSLLISW EYKVHPYRYY RITYGETGGN SPVQEFTVPS VLSTAEISGL 780
781 KPGVDYTITV YAVTRGVDSA PISINYRTPG GGGSGGGGSG GGGSGGGGTI AEYAARIEAL 840
841 IRAAQEQQEK NEAALRELYK WAS
```

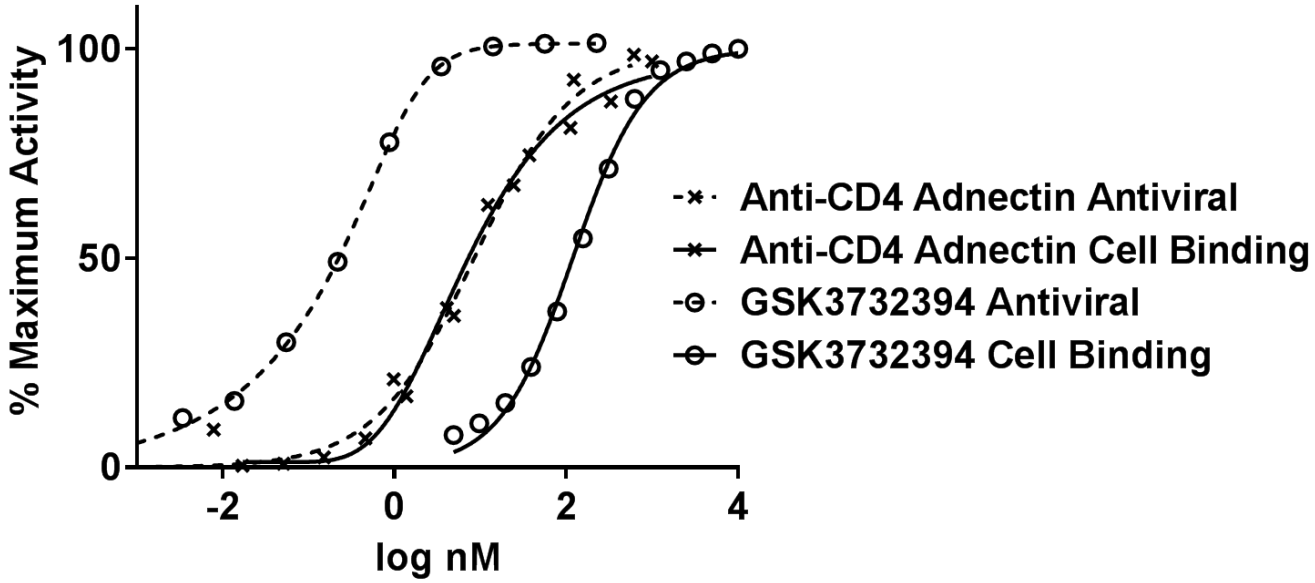

Virus	Passage Number	Days	Fold Change	T63	T138	N301	F394	S401	L544	Q577
NL_{4-3} wt	37	175	1	T	T	N	F	S	L	Q
Selected virus	37	175	18	I	I	K	S	T	S	R
Recombinant virus	-	-	60	I	I	K	S	T	S	R